SIMULATION OF SEMICONDUCTOR DEVICES AND PROCESSES Vol. 4
Edited by W. Fichtner, D. Aemmer - Zurich (Switzerland) September 12-14, 1991 - Hartung-Gorre

Physical Modelling of Transport Parameters for Strained Layer p - $Si_{1-x}Ge_x$ Devices*

T. Manku and A. Nathan
Electrical and Computer Engineering, University of Waterloo
Waterloo, Ontario, CANADA N2L 3G1.

Abstract

The density of states effective mass and the carrier concentration effective mass have been computed for strained SiGe for various Ge fractions, x. The computations take into account the effects of spin orbit coupling due to the inherently high strain involved. A generic expression of the valence band structure of any semiconductor under strain has been developed, based on which we have computed the various scattering relaxation times, viz., acoustic, optical, and alloy, for subsequent mobility calculations. The resulting mobility which turns out to be a tensor, is presented for various Ge fractions under strained and unstrained conditions.

I. Introduction

A new and promising material in the area of semiconductor devices is the strained SiGe alloy. The strain is a consequence of the difference in lattice constants between the SiGe and <001> Si substrate it is grown on. This inherent strain results in favourable electronic transport and optical properties [1] (i.e. higher mobility and a reduction in band gap), making SiGe very attractive for fabrication of high performance transistors such as MODFETs, heterojunction bipolar transistors, resonant tunneling diodes, and most importantly, optoelectronic devices for long wavelength applications [2]. In view of the desirable electronic properties of strained SiGe, adequate physical models have to be developed for realistic simulation of SiGe based devices. The starting point in physical parameter modeling is a study of the band structure. With knowledge of the energy spectrum of strained SiGe, physical parameters such the band gap, effective mass, the effective density of states as well as the density of states, can be obtained. Furthermore, the energy spectrum allows calculation of the scattering relaxation times and subsequently, the carrier mobility.

In this paper, we first examine the effects of strain on the valence band for any semiconductor in general, and present a generic expression which includes the effects of spin-orbit coupling. This is subsequently applied to the SiGe alloy system, and the density of state (DOS) effective mass as well as the free carrier concentration (CC) effective mass are computed. A systematic calculation of the

* this work was funded by the Natural Sciences and Engineering Research Council (NSERC) of Canada and the Federal Network Centres of Excellence in Microelectronics (NCE Micronet).

various lattice scattering relaxation times is then shown; the most important being acoustic, optical, and alloy. An effective relaxation time is then obtained using Mathiessen's rule, from which we obtain the lattice mobility based on the first order expansion of the Boltzmann's transport equation. In view of the inherently large strain, the band structure reduces from 3-fold to 2-fold symmetry resulting in a tensorial mobility.

II. Valence Band Structure Under Strain

The effect of strain on the valence band was first presented by Pikus and Bir [3]. They obtained a closed form expression of the band structure, which was derived by taking a first order perturbation about the strain tensor $\varepsilon = 0$ in the one electron Schroedinger equation, viz.,

$$\left[-\frac{\hbar^2}{2m_e} \nabla^2 + V_o(\mathbf{r}) \right] U^o_{\mathbf{k}\,j} = E^o_{\mathbf{k}} U^o_{\mathbf{k}\,j}\,, \tag{1}$$

where m_0 is the mass of the electron, $\hbar$ denotes Planck's constant divided by 2π, $V_0(\mathbf{r})$ is the periodic potential of the unstrained unit cell, $E^o_{\mathbf{k}}$ is the energy spectrum of the unstrained material, and $U^o_{\mathbf{k}\,j}$ is the unstrained degenerate electron wave function transforming according to the representation Γ^+_{25} (i.e. j= yz,zx,xy).

In their equation [3], however, the effects of spin orbit coupling were ignored. In strained SiGe, typical strain levels are of the order of thousands of atmospheres. In view of this large strain, it becomes clear that the effects of spin orbit coupling have to be included in order to obtain a more accurate representation for the valence band structure of $Si_{1-x}Ge_x$. To include spin-orbit coupling one needs to consider a set of degenerate basis functions (1,0) (spin-up) and (0,1) (spin down) as well as the k-independent spin orbit perturbation matrix [4]. By using this approach, we obtain the following expression for the valence band structure applicable to all strained semiconductors,

$$\sum_{j=0}^{3} \sum_{i=0}^{3-j} a_{ji}(\theta,\phi,\varepsilon) E^i_k k^{2j} = 0, \tag{2}$$

where polar coordinates, k, ϕ, θ have been employed. The components a_{ij} are functions of the deformation potentials, the band parameters, θ and ϕ, and the strain elements. A comprehensive treatment of the above approach will be presented elsewhere. Equation (2) yields three distinct values of E_k for a particular value of k; each of which corresponds to the so called heavy hole (HH), light hole (LH), and spin-off (SO) bands. The splitting of the valence bands due to strain can be calculated using equation (2) by setting k = 0. Solutions to equation (2) for either $E_k(k)$ or $k^2(E_k)$ can

be obtained by a trigonometric method. In calculating the band structure of SiGe, we assumed that the band parameters varied from Si to Ge in accordance to the results obtained by Lawaetz [5].

In Figs. (1) and (2), a plot of the energy spectrum and a cross sectional view of a constant energy surface is given for the HH and LH bands of pure silicon and strained SiGe (the composition of Ge being 0.3) [6]. The HH band moves upwards due the strain and becomes asymmetric in the xz and xy planes. From Fig. (1b), we can deduce that the tensorial effective mass in the k_z direction is larger than the corresponding mass in the k_y (or the k_x) direction. This in turn produces a lower mobility in the z-direction compared with the y- or x-directions. The same applies for the LH band (see Fig. 2b). The key difference in the two bands (LH and HH) is that the LH band moves downwards and the HH band moves upwards (see Figs. 1a and 2a).

III. Effective Masses

The density of states effective (DOS) mass provides a convenient way of describing the the mass of a carrier that is needed to produce the correct density of states when compared to the ideal free carrier relationship [7]. By comparing the DOS effective mass for strained p-type SiGe to that of one with a spherical parabolic band structure, the following expression for the DOS effective mass is obtained,

$$\frac{m_{DOS}(E)}{m_o} = \left[\frac{1}{2\pi\sqrt{E}}\frac{dV}{dE}\right]^{2/3}\left(\frac{\hbar^2}{2m_o}\right), \tag{3}$$

where dV/dE is the change in volume dV in k-space for a change in energy dE.

Selected results for the DOS effective mass are shown in Fig. 3 for the following Ge compositions: 0%, 5%, 10% , 20%, and 30%. For both HH and LH bands, the DOS effective mass becomes lower as the Ge composition increases, leading to an increase in the mobility. The lowering of the DOS effective mass is mainly due to the strain and not due to the interaction of the Si atoms with the Ge atoms.

The carrier concentration effective masses, $m_{CC}(T)$ for the valence bands in SiGe as a function of temperature, T is next calculated using,

$$m_{CC}^{3/2}(T) = \frac{2}{\sqrt{\pi}}\beta^{3/2}\int_0^\infty E^{1/2}m_{DOS}^{3/2}(E)\exp(-\beta E)dE, \tag{4}$$

which was derived using Maxwell Boltzmann's statistics. Here, k_B is Boltzmann's constant and $\beta = (k_B T)^{-1}$. Note that the nonparabolicity of the band structure is accounted for by $m_{DOS}(E)$. In Fig. (3), results of the CC effective mass as a function of temperature for various Ge fractions are shown

for the HH and LH bands. As the Ge fraction increases, the corresponding strain increases thus producing a decrease in the CC effective mass. The total CC effective mass, viz.,

$$m_{CC,total} = (m_{CC,1}^{3/2} + m_{CC,2}^{3/2})^{2/3}, \tag{5}$$

is shown in Fig. 4. Note that at high temperatures, the total CC effective mass becomes virtually temperature independent. In Fig. 5, results of the CC effective mass as a function of Ge composition are given for two widely used device temperatures. Note that there is a significant reduction in the CC effective mass as the Ge fraction increases. For pure silicon (x = 0) we reproduce the well known results at 300 K, i.e. $m_{CC,total} = 1.1\, m_o$. At x = 30%, there is a dramatic reduction in the CC effective mass. Relative to Si (x = 0), the mass is lowered by a factor of three.

IV. Mobility

The three major scattering relaxation times that will be considered are non-polar optical, acoustic phonon, and alloy. To simplify the expressions for the relaxations times, we make the following assumptions: (i) acoustic phonon scattering is perfectly elastic, (ii) optical phonon scattering occurs inelastically, (iii) the holes scatter isotropically, (iv) alloy scattering is independent of temperature, and (v) the relaxation times are only functions of energy and do not depend explicitly on **k** (i.e. the overlap integral is unity).

In acoustic phonon scattering, energy and momentum conservation restricts intra-valley scattering by acoustic phonons to long-wavelength modes. Such modes cannot change the energy of an electron other than through the elastic strain associated with them. A long-wavelength acoustic displacement cannot effect the energy since neighboring unit cells all move by almost the same amount; only differential displacement, namely the strain is of importance. Using deformation potential theory and by defining an effective deformation potential, E_{eff} for the valence band, the total acoustic phonon scattering relaxation time, τ_{ac} is given by

$$\frac{1}{\tau_{ac}} = \frac{\pi k_B T E_{eff}^2}{\hbar \rho u_l^2} N(E), \tag{6}$$

where N(E) is the total density of states in the valence bands, ρ is the material density, and u_l is the velocity of sound in the material. In the above equation, we assume that the scattering of holes in each sub-band contributes to the relaxation time independently.

As in the case of acoustic phonon scattering, energy and momentum conservation restricts intra-valley scattering by optical phonons to long-wavelength modes. However, unlike the case of acoustic phonons, long wavelength optical displacement may effect the electronic energy directly.

Optical phonons have a characteristic frequency, ω_0 which is independent of it's wave vector, whereas in the case of acoustic phonons, the frequency is found to be linearly related to the wave vector. By defining an optical phonon coupling constant D_tK, the relaxation time due to optical phonons is given by the following expression,

$$\frac{1}{\tau_{op}^{i}} = \frac{\pi D_t K^2}{2\rho\omega_0} [\, n(\omega_0)\, N_i(E + \hbar\omega_0) - (n(\omega_0) + 1)\, N_i(E - \hbar\omega_0)\,], \tag{7}$$

where $n(\omega_0)$ is the Bose-Einstein phonon distribution with optical phonon frequency, ω_0. In Eqn. (7), the first and second terms represent the creation and annihilation of a phonon. Since each sub-band (i.e. HH, LH and SO bands) can scatter a hole into any other sub-band, providing that the density of states of that sub-band is non-zero, the total optical scattering relaxation time is given by the following sum,

$$\frac{1}{\tau_{op}^{T}} = \sum_{i=1}^{3} \frac{1}{\tau_{op}^{i}}. \tag{8}$$

In alloy scattering, the fluctuations from uniformity give rise to local changes in the Coulombic potential experienced on the average by the hole, and hence to scattering. Since these fluctuations should be independent of temperature, the alloy scattering relaxation time should also be independent of temperature, viz.,

$$\frac{1}{\tau_{alloy}^{i}} = \frac{\pi}{\hbar} U^2\, \Omega\, x\, (1 - x)\, N_i(E), \tag{9}$$

where U is the interaction potential, Ω is the volume of the cubic cell, and x as usual denotes the Ge fraction. The interaction potential has various interpretations. It can be taken as the difference in band gap of the two components in binary compounds, or the difference in their electron affinities. So it is probably prudent to regard U as a quantity that has to be determined empirically.

The relaxations times discussed above were combined using the Mathiessen's rule, resulting in an effective relaxation time, $\tau(E)$. Using $\tau(E)$, the mobility of strained SiGe is then calculated using the following form,

$$\mu_{ij} = \frac{\frac{e}{\hbar^2} \int d^3\mathbf{k}\, \tau(E) \frac{\partial E}{\partial k_i} \frac{\partial E}{\partial k_j} \frac{\partial f}{\partial E}}{\int d^3\mathbf{k}\, f(E, E_f, T)}, \tag{10}$$

which is based on a first order expansion of the Boltzmann's transport equation. In Eqn. (10), μ_{ij} denotes the mobility tensor, e is the elementary charge, k_i are the components of **k** (i, j = x, y, z), E is the hole energy, E_f is the Fermi-level, T is temperature, and f (E, E_f, T) = exp ([E - E_f]/T). Since the energy spectrum of the valence band is found to have only 2-fold symmetry, the mobility becomes a tensor taking the following form,

$$\mu_{\mathbf{p}} = \begin{bmatrix} \mu_{xx} & 0 & 0 \\ 0 & \mu_{xx} & 0 \\ 0 & 0 & \mu_{zz} \end{bmatrix}, \tag{11}$$

where $\mu_{xx} = \mu_{yy}$ only when x = 0 (i.e. at zero strain, $\varepsilon = 0$). This result requires one to solve the drift-diffusion equation in the following tensorial form, $\mathbf{j} = - q\, p\, \mu_{\mathbf{p}} \cdot \text{grad}\, \phi_p$.

The values of the various parameters used in our mobility calculations are shown in Table I. Parameter values that are not known for SiGe, have been determined using a linear interpolation between the values of Si and Ge. The value of the alloy interaction potential was chosen such that our calculated results fit the trends of measurement data of Hall mobility in unstrained SiGe [8]. We have only considered the mobility at 300 K. At lower temperatures, the Ge atom acts like an impurity in Si (activation energy ~ 0.5 eV) and this can be attributed to the fact Si has a larger electron affinity than Ge.

TABLE I: Parameters used in calculations.

Parameters	Units	Silicon	Germanium
E_{eff}	eV	5.2	6.9
D_tK	eV/cm	6.6×10^8	5.9×10^8
U	eV	0.27	0.27

Results of the mobility of strained and unstrained SiGe at 300 K are shown in Fig. 7. We indeed recover the results of the unstrained lattice hole mobilities of Si and Ge (i.e. x = 0.0 and x = 1.0, respectively). Under strained conditions, the distortion in the band structure introduces anisotropies in the mobility, which results in a tensorial mobility with an in-plane component (parallel to surface of the crystal) and a component along the growth plane. We note that the strain drastically increases the mobility, with the in-plane mobility component being significantly larger than the perpendicular counterpart. This can be better understood with Figs. 1 and 2; the cross section energy spectrum shows a larger effective mass in the z-direction compared with that of the y- or x-directions.

Empirical relations describing the hole lattice mobility components at room temperature were determined to be as follows:

$$\mu_{xx} = \mu_{Si} \exp[x\, \alpha_{xx}(x)] ,$$

$$\mu_{zz} = \mu_{Si} \exp[x\, \alpha_{zz}(x)] , \qquad (12)$$

where μ_{Si} = 459 cm^2/Vs and the α's are fourth order polynomials which are functions of the Ge fraction, x. The coefficients of the respective α's are listed below in Table II.

TABLE II: Coefficients for α_{xx} and α_{zz} .

Degree	α_{xx}	α_{zz}
4	35.1904	40.2994
3	-78.1230	-89.5728
2	59.5064	67.0455
1	-15.4922	-17.4045
0	2.8737	2.6027

V. Conclusions

By incorporating the effects of spin-orbit coupling into the strained valence band structure, we compute the DOS and CC effective mass as well and the scattering relaxation times associated with optical, acoustic, and alloy scattering mechanisms. The resultant lattice mobility of holes is then computed, and is found to be a tensor due to the strain-induced anisotropies in the band structure. We are currently incorporating the effects of impurity scattering on mobility.

REFERENCES

[1] R. People, IEEE J. Quantum Electronics **QE-22**, 1696 (1986).

[2] S. S. Iyer, G. L. Patton, J. M. C. Stork, B. S. Meyerson, and D. L. Harame, IEEE Trans. Electron **ED-36**, 2043 (1989).

[3] G. E. Pikus and G. L. Bir, Sov. Phys. - Solid State **1**, 1502 (1959).

[4] E. O. Kane, Phys. Chem. Solids **1**, 82 (1956).

[5] P. Lawaetz, Phys. Rev. B **4**, 3460 (1971).

[6] T. Manku and A. Nathan, Phys. Rev. B **43**, (1991) in press.

[7] T. Manku and A. Nathan, J. Appl. Phys. **69**, (1991) in press.

[8] A. Levitas, Phys. Rev. **99**, 1810 (1955).

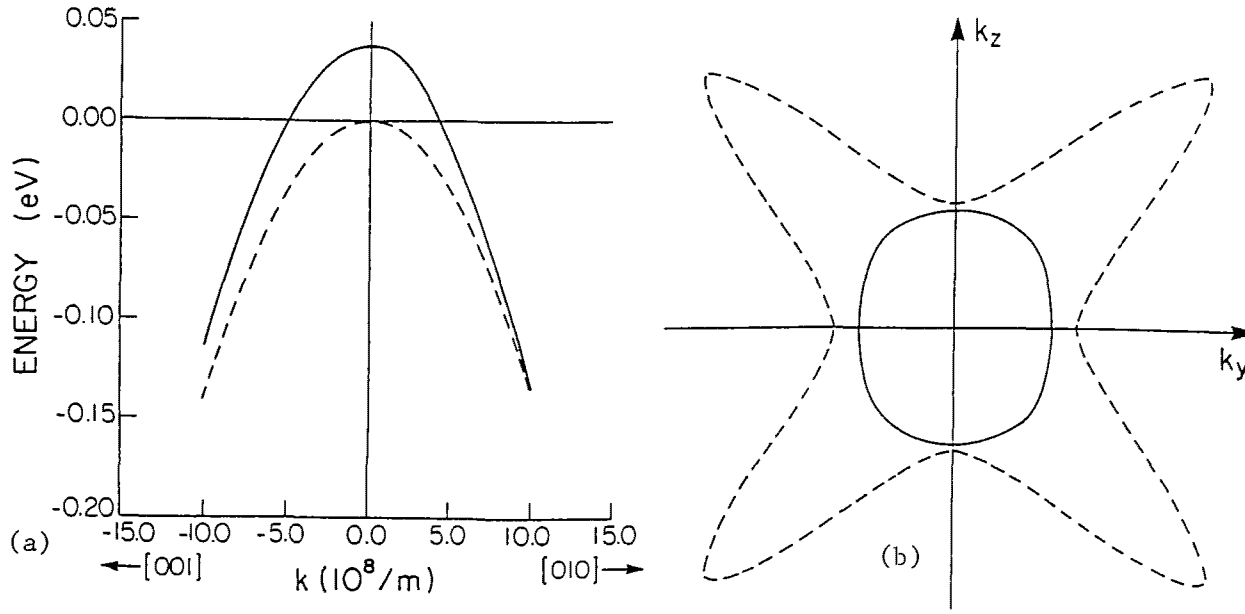

Fig 1. (a) Spectrum of the HH band in the k_y and k_z directions.

(b) Cross-section of an energy band shell in the k_y-k_z plane; dashed line represents Si (x = 0.0) and the solid line SiGe (x =0.3).

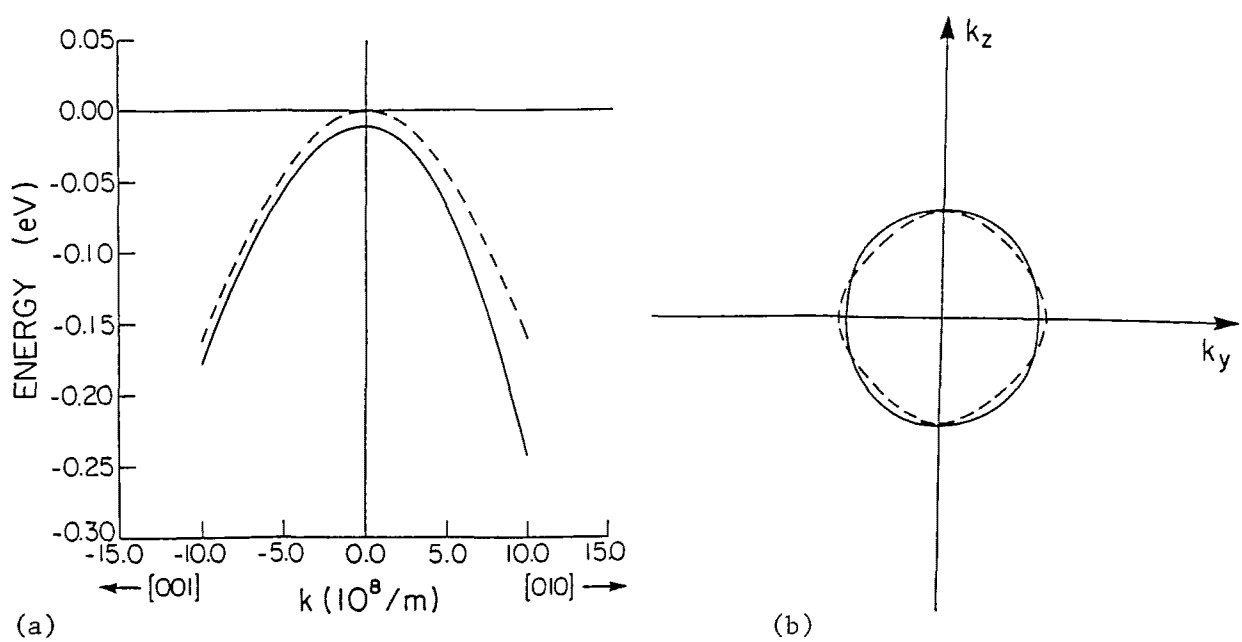

Fig 2. Same as Fig.1, but for the LH band.

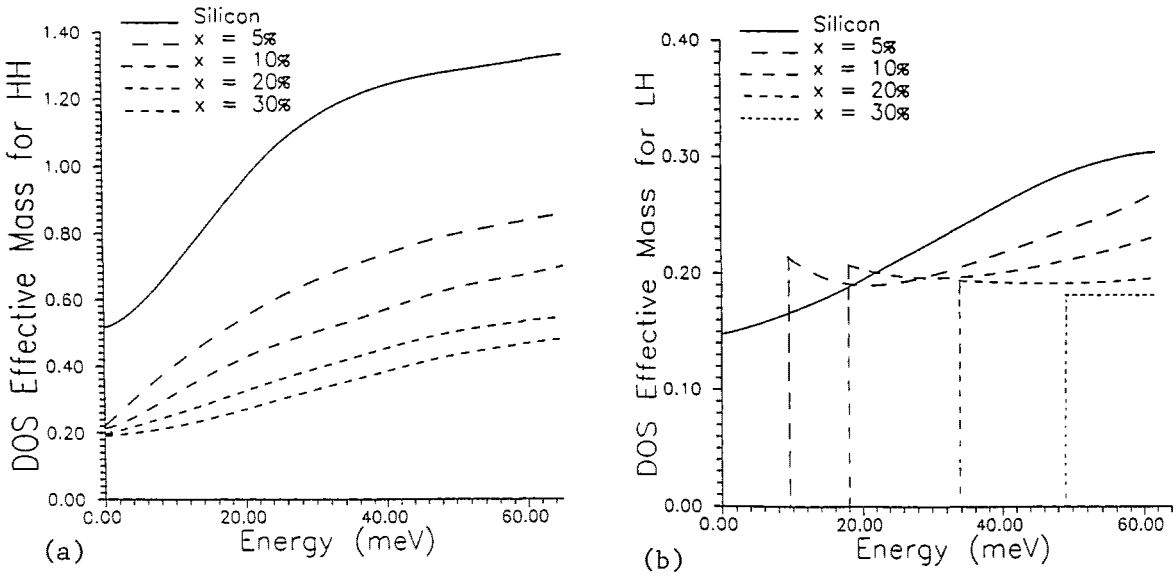

Fig 3. (a) DOS effective mass (normalized with m_0) for the HH band in SiGe.
(b) DOS effective mass for the LH band.

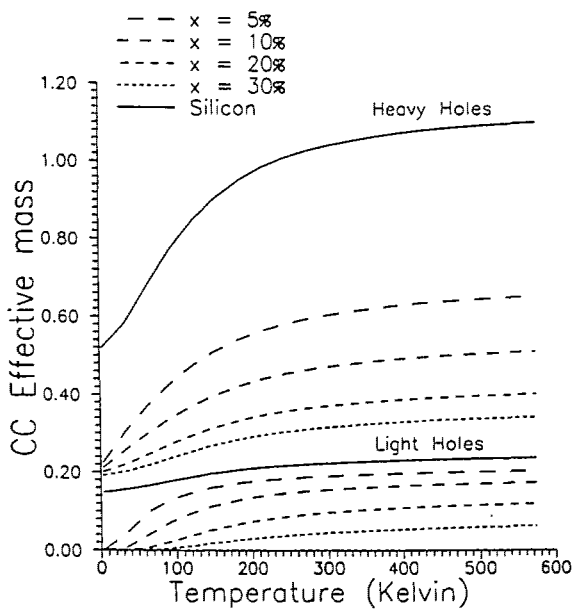

Fig 4. The normalised CC effective mass for heavy holes and light holes as a function of temperature.

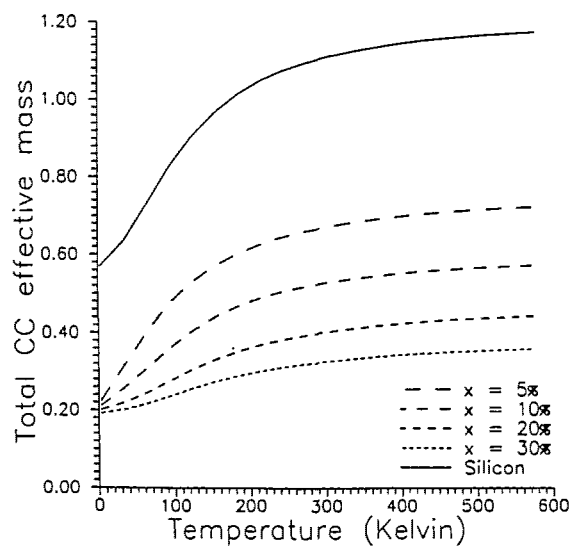

Fig 5. Normalised total CC effective mass as a function of temperature.

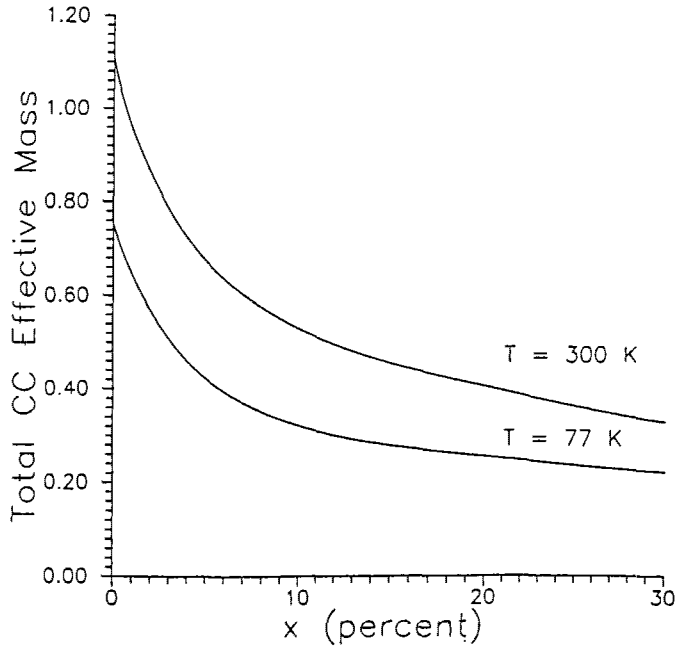

Fig 6. CC effective mass for T= 77 K and T = 300 K as a function of Ge fraction.

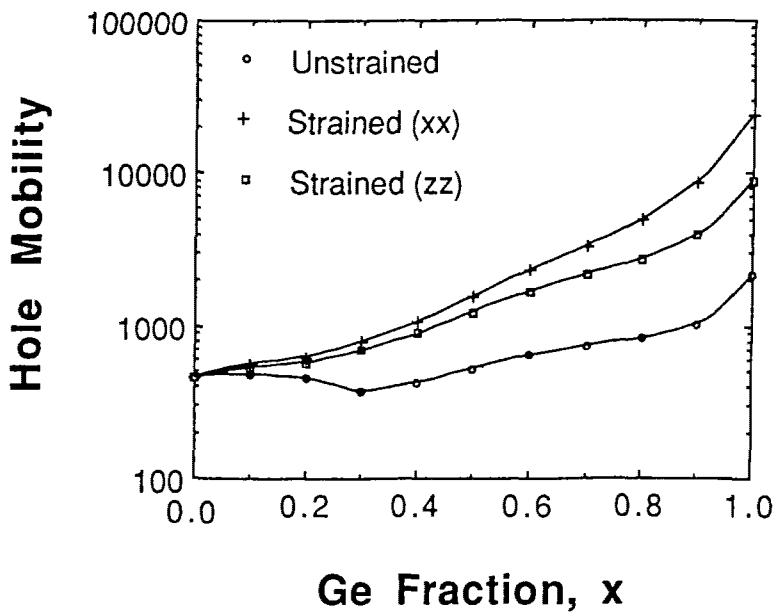

Fig 7. Mobility as a function of Ge fraction at 300 K for unstrained and strained SiGe. Under strain, the mobility splits into two different components, μ_{xx} and μ_{zz}.